Proteome-wide identification of NEDD8 modification sites reveals distinct proteomes for canonical and atypical NEDDylation

Sofia Lobato-Gil, Jan B Heidelberger, Chantal Maghames, Aymeric Bailly, Lorene Brunello, Manuel Rodriguez, Petra Beli, Dimitris P Xirodimas

Cell Reports

Report

Proteome-wide identification of NEDD8 modification sites reveals distinct proteomes for canonical and atypical NEDDylation

Graphical Abstract

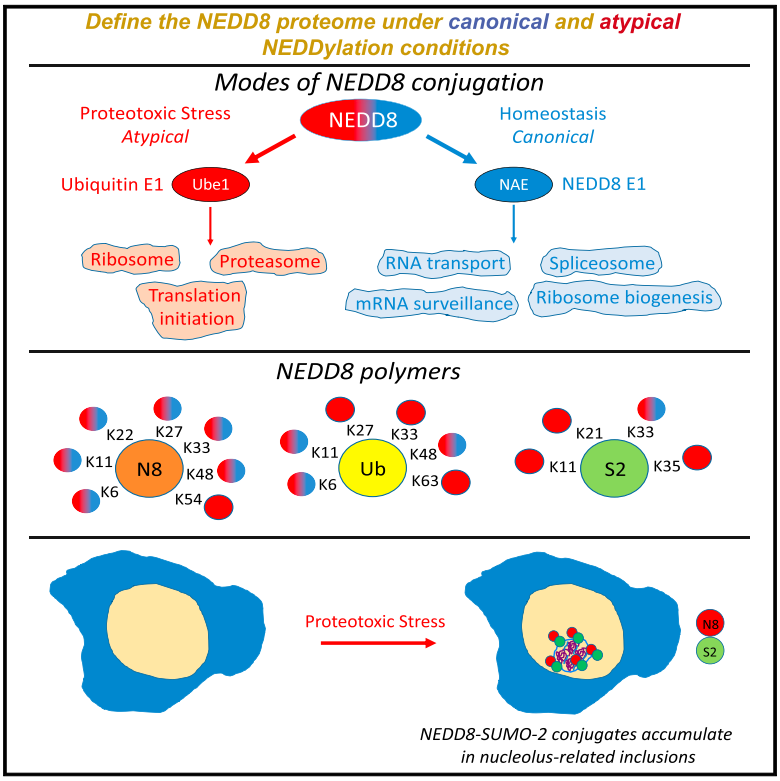

Highlights

- A diGly-based approach for the proteome-wide identification of NEDD8 modification sites
- Distinct proteomes for canonical and atypical NEDDylation
- Existence of diverse poly-NEDD8, hybrid NEDD8-ubiquitin, and NEDD8-SUMO-2 polymers
- NEDD8-SUMO-2 chains accumulate in nucleolus-related inclusions upon proteotoxic stress

Authors

Sofia Lobato-Gil, Jan B. Heidelberger, Chantal Maghames, ..., Manuel S. Rodriguez, Petra Beli, Dimitris P. Xirodimas

Correspondence

dimitris.xirodimas@crbm.cnrs.fr (D.P.X.), p.beli@imb-mainz.de (P.B.)

In Brief

Identification of modification sites for ubiquitin/Ubls is critical for elucidating the regulated processes. Lobato-Gil et al. report the proteome-wide identification of NEDD8 sites, which defines distinct NEDD8 proteomes for canonical and atypical NEDDylation and formation of diverse homo- and hybrid NEDD8 polymers. Proteotoxic-stress-induced NEDD8-SUMO-2 chains accumulate in nucleolus-related inclusions.

Lobato-Gil et al., 2021, Cell Reports *34*, 108635
January 19, 2021
https://doi.org/10.1016/j.celrep.2020.108635

CellPress

Cell Reports

CellPress
OPEN ACCESS

Report

Proteome-wide identification of NEDD8 modification sites reveals distinct proteomes for canonical and atypical NEDDylation

Sofia Lobato-Gil,[1] Jan B. Heidelberger,[2] Chantal Maghames,[1] Aymeric Bailly,[1] Lorene Brunello,[1] Manuel S. Rodriguez,[3,4] Petra Beli,[2,*] and Dimitris P. Xirodimas[1,5,*]

[1]CRBM, University of Montpellier, CNRS, Montpellier, France
[2]Institute of Molecular Biology (IMB), Mainz, Germany
[3]Laboratoire de Chimie de Coordination (LCC), UPR 8241, CNRS, Toulouse, France
[4]IPBS-University of Toulouse III-Paul Sabatier, Toulouse, France
[5]Lead Contact
*Correspondence: dimitris.xirodimas@crbm.cnrs.fr (D.P.X.), p.beli@imb-mainz.de (P.B.)
https://doi.org/10.1016/j.celrep.2020.108635

SUMMARY

The ubiquitin-like molecule NEDD8 controls several biological processes and is a promising target for therapeutic intervention. NEDDylation occurs through specific NEDD8 enzymes (canonical) or enzymes of the ubiquitin system (atypical). Identification of NEDD8 sites on substrates is critical for delineating the processes controlled by NEDDylation. By combining the use of the NEDD8 R74K mutant with anti-di-glycine (anti-diGly) antibodies, we identified 1,101 unique NEDDylation sites in 620 proteins. Bioinformatics analysis reveals that canonical and atypical NEDDylation have distinct proteomes; the spliceosome/mRNA surveillance/DNA replication and ribosome/proteasome, respectively. The data also reveal the formation of poly-NEDD8, hybrid NEDD8-ubiquitin, and NEDD8-SUMO-2 chains as potential molecular signals. In particular, NEDD8-SUMO-2 chains are induced upon proteotoxic stress (atypical) through NEDDylation of K11 in SUMO-2, and conjugates accumulate in previously described nucleolus-related inclusions. The study uncovers a diverse proteome for NEDDylation and is consistent with the concept of extensive cross-talk between ubiquitin and Ubls under proteotoxic stress conditions.

INTRODUCTION

Modification of proteins with the ubiquitin-like molecule NEDD8 controls both homeostatic and stress-related processes and with the exception of *S. cerevisiae*, NEDD8 is essential in all tested organisms (Abidi and Xirodimas, 2015; Enchev et al., 2015). Protein NEDDylation follows a pathway similar to that of ubiquitin/Ubl conjugation and involves the activity of E1, E2, and E3 enzymes that lead to the covalent modification of NEDD8 to the ε amino group of a lysine residue of the target. The heterodimer E1 UBA3/APPBP1 (NAE), E2 conjugating enzymes UBE2M (UBC12) and UBE2F, and multiple E3 ligases promote NEDD8 conjugation on substrates (Abidi and Xirodimas, 2015; Enchev et al., 2015). The activity of deNEDDylating enzymes removes NEDD8 from targets, ensuring that the process is reversible. The COP9 signalosome that deNEDDylates the cullin family of proteins and NEDP1 (DEN1/SENP8) are the two specific deNEDDylating enzymes (Abidi and Xirodimas, 2015; Enchev et al., 2015). The aforementioned components define the so-called canonical pathway that mainly operates under homeostatic conditions. In addition to the cullin family of proteins, several non-cullin substrates have been reported as potential targets for the canonical NEDD8 pathway, involved in the control of the cell cycle, transcription, subcellular localization, nucleolar signaling, DNA damage response, neuronal maturation, and synaptic plasticity (Abidi and Xirodimas, 2015; Brockmann et al., 2019; Enchev et al., 2015; Vogl et al., 2015).

In addition to this mode of NEDDylation, NEDD8 can be activated by the ubiquitin E1 enzyme UBA1 (UAE/UBE1) and conjugated onto substrates by enzymes of the ubiquitin system (Hjerpe et al., 2012; Leidecker et al., 2012). This mode that defines the atypical pathway is mainly observed under proteotoxic stress conditions. It is characterized by the formation of hybrid NEDD8-ubiquitin chains, which impact on the ubiquitin proteasome system (UPS) and nuclear protein aggregation (Leidecker et al., 2012; Li et al., 2015; Maghames et al., 2018). However, it is still unclear whether these two modes of NEDDylation use a shared or unique proteome to transmit biological outcome.

Critical information that allows the definition of biological processes controlled by the ubiquitin/Ubl pathways is the identification of modification sites on substrates. A breakthrough in the ubiquitin/Ubl research has been the development of antibodies that specifically recognize the di-glycine (diGly) remnant left on modified lysine residues upon trypsin digestion. This approach has allowed the identification of over 50,000 sites, which, however, does not distinguish between ubiquitin, NEDD8, or ISG15

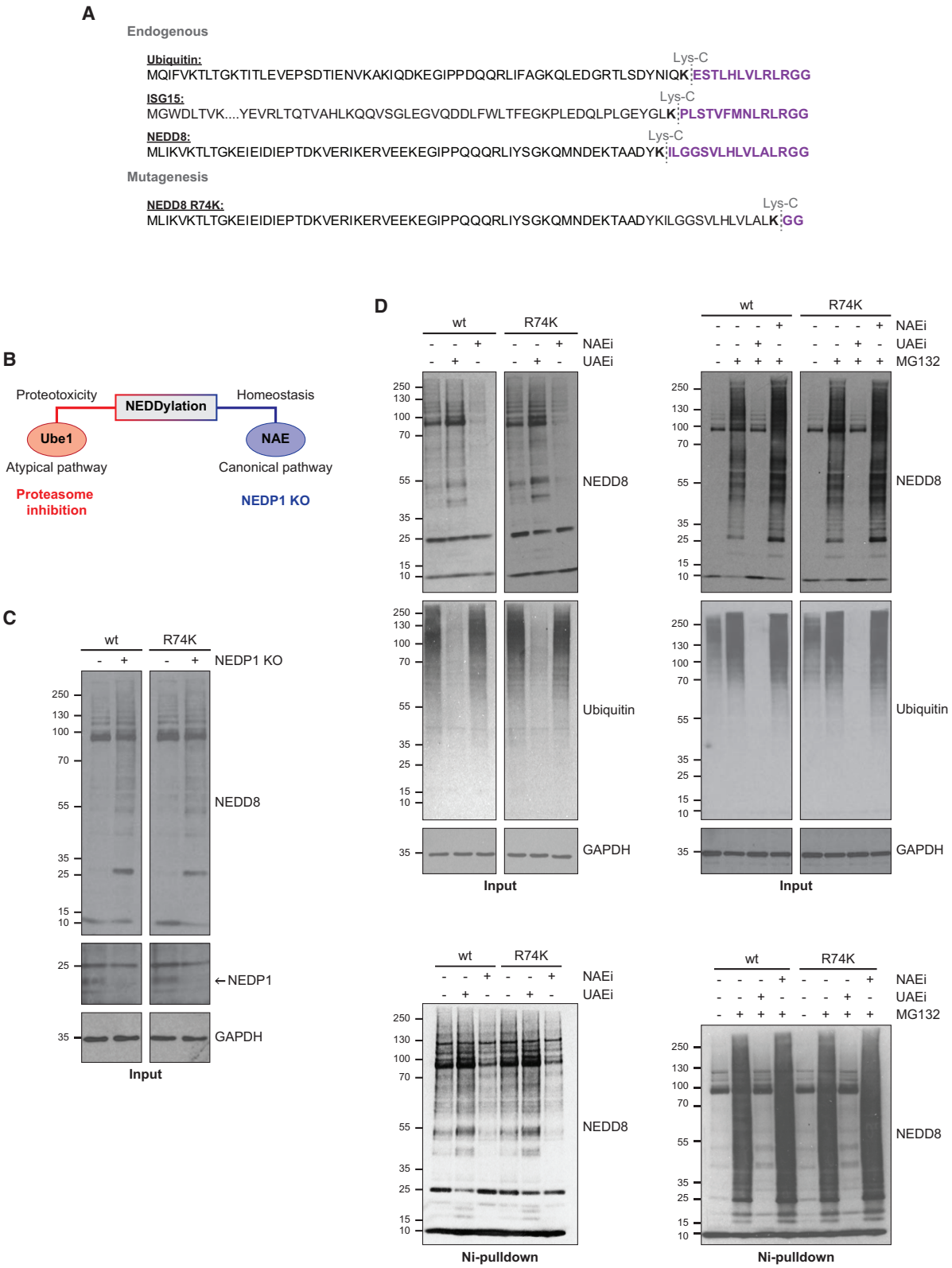

(legend on next page)

conjugation, as all these modifications provide a diGly remnant upon trypsin digestion (Kim et al., 2011; Ordureau et al., 2015; Wagner et al., 2011; Xu et al., 2010).

In order to identify proteome-wide NEDDylation sites, we applied a strategy that relies on the use of the NEDD8^{R74K} mutant in combination with anti-diGly antibodies (Vogl et al., 2020). We characterized both the canonical and atypical NEDD8 proteomes and identified, in total, 1,101 NEDDylation sites on 620 proteins. A striking finding is the existence of distinct proteomes for canonical and atypical NEDDylation, indicating that the two modes of NEDDylation are functionally discrete. Another interesting finding is the NEDDylation of almost all available lysines on NEDD8 and ubiquitin and many on SUMO-2, indicative of the existence of multiple and distinct poly-NEDD8 and hybrid NEDD8-ubiquitin, NEDD8-SUMO-2 chains. In particular, NEDD8-SUMO-2 chain formation, mainly through K11 on SUMO-2, is specifically induced upon atypical NEDDylation conditions (proteotoxic stress). The stress-induced NEDD8-SUMO-2 conjugates accumulate in previously described nucleolus-related inclusions, consistent with a role of NEDD8-SUMO-2 hybrid chains in protein quality control. Collectively, the study reveals an extensive proteome for the NEDD8 pathway, including the formation of diverse polymers as potential molecular signals.

RESULTS

The use of the NEDD8^{R74K} mutant as a tool to identify NEDDylation sites

The development of the anti-diGly antibodies has been a revolution in the ubiquitin/Ubl field, as it allows the proteome-wide identification of modification sites on substrates (Kim et al., 2011; Ordureau et al., 2015; Wagner et al., 2011; Xu et al., 2010). However, a key handicap of these tools is that they do not allow the discrimination between ubiquitin, NEDD8, or ISG15 modification sites, as all these modifiers provide a diGly signature on modified peptides upon trypsin digestion. We sought to develop an approach that would allow the use of the anti-diGly antibodies to specifically isolate NEDDylated peptides for the proteome-wide identification of NEDDylation sites. For this, we generated HCT116 colon cancer cell lines stably expressing the 6His-NEDD8^{R74K} mutant. We used infection conditions that establish endogenous levels of expression of the ectopic NEDD8 construct (Liu and Xirodimas, 2010) (Figure S1A). The use of the endopeptidase LysC instead of trypsin would specifically generate diGly remnants only in NEDD8^{R74K} but not in ubiquitin or ISG15 modified proteins (Figure 1A). This allows the use of anti-diGly antibodies to isolate peptides with NEDD8^{R74K}-derived diGly remnants and the proteome-wide identification of NEDDylation sites. A similar approach has been successfully used for the identification of SUMOylation sites and, more recently, of NEDDylation sites, but only under canonical conditions (Tammsalu et al., 2014; Vogl et al., 2020).

We used this system to identify NEDDylation sites under canonical and atypical NEDDylation conditions (Figure 1B). For the canonical pathway, we used HCT116 cells deleted of the de-NEDDylating enzyme NEDP1 that results in dramatic increase of global NEDDylation that strictly depends on the canonical, but not atypical, NEDD8 pathway (Bailly et al., 2019) (Figure 1B; Figure S1B). For the identification of NEDD8 sites under atypical conditions, we treated cells with the proteasome inhibitor MG132, which results in the increase of NEDDylation that strictly depends on enzymes of the ubiquitin system (Hjerpe et al., 2012; Leidecker et al., 2012) (Figure 1B; Figure S1B). We confirmed that the NEDD8^{R74K} mutant provides a NEDDylation profile similar to that of wild-type NEDD8 (Figure 1C) and follows the characteristics of canonical and atypical endogenous NEDDylation; namely, that the increase in NEDDylation upon NEDP1 deletion depends on NAE but not on UAE (ubiquitin-activating enzyme) and, conversely, that the increase in NEDDylation upon MG132 treatment depends on UAE but not on NAE (Figure 1D; Figure S1B).

Distinct proteomes for canonical and atypical NEDDylation

Cell extracts from canonical and atypical NEDDylation conditions were used for LysC digestion, immunoprecipitation of peptides with anti-diGly antibodies before fractionation, and liquid chromatography-tandem mass spectrometry (LC-MS/MS) analysis (Figure 2A; STAR Methods). From 2 independent experiments, we identified, in total, 880 sites on 489 proteins under canonical NEDDylation conditions and 272 sites in 189 proteins under atypical NEDDylation conditions (Figure 2B; Table S1). Many sites on previously characterized NEDD8 substrates were identified, including cullin 3, UBA3/APPBP1, Ubc12, ribosomal proteins, and histones, indicating the validity of the approach (Li et al., 2014; Ma et al., 2013; Mergner et al., 2015; Xirodimas et al., 2008) (Figure S2; Table S1). Modification sites for additional well-established NEDD8 substrates (members of the cullin family) were identified but were not included in further analysis, as their localization probability was below the set threshold (STAR Methods). By combining results from both atypical and canonical conditions, we identified, in total, 1,101 unique NEDD8 sites in 620 proteins. 51 sites were identified in both conditions, whereas 829 sites on 431 substrates were specific for canonical NEDDylation, and 221 sites on 131 substrates were specific for atypical NEDDylation (Figure 2B; Table S2). This indicates that the two modes of NEDDylation have a rather distinct proteome and modification profile. Interestingly, 58 substrates were identified under both modes of NEDDylation but

Figure 1. Use of the NEDD8^{R74K} mutant to identify NEDDylation sites

(A) Sequence alignment of ubiquitin, ISG15, and NEDD8 showing the cleavage site for endopeptidase Lys-C. The R74K mutation in NEDD8 allows the generation of a diGly remnant only on NEDDylated proteins.

(B) Schematic representation of the conditions used to enhance canonical (NEDP1 knockout) and atypical (MG132 treatment) mode of NEDDylation.

(C) Western blot analysis of extracts from parental or NEDP1 knockout (C8) HCT116 cells stably expressing either wild-type 6His-NEDD8 or 6His-NEDD8^{R74K} mutant.

(D) Cells described in (C) were either untreated or treated with MG132 (30 μM, 4 h), NAE inhibitor (MLN4924, 1 μM, 5 h), or UAE inhibitor (MLN7243, 0.5 μM, 5 h) as indicated. Total cell extracts and isolated 6His-NEDD8 conjugates were used for western blot analysis.

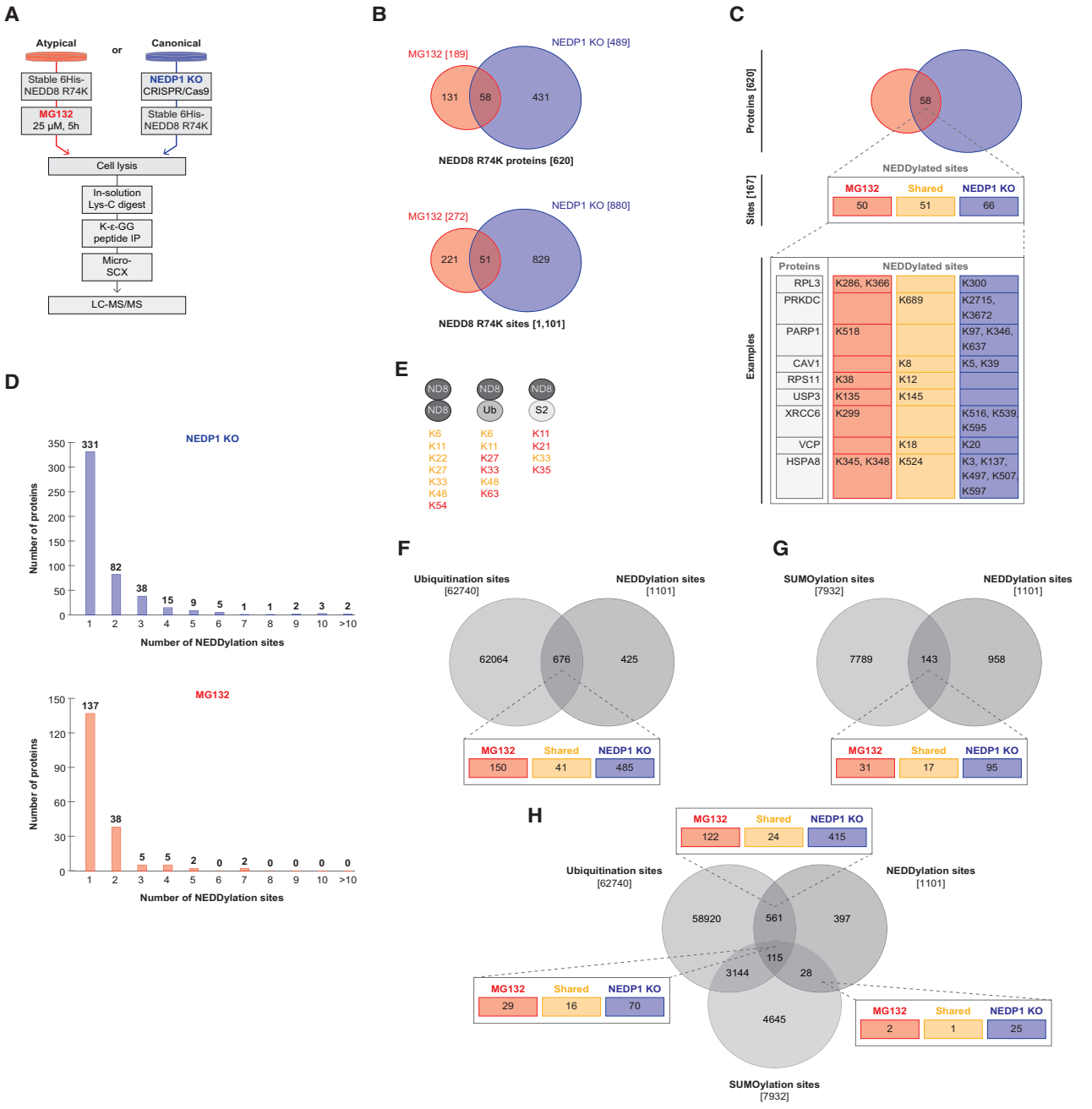

Figure 2. Distinct proteomes for canonical and atypical NEDDylation. Formation of diverse homotypic and heterotypic NEDD8 polymers

(A) Schematic representation of the strategy used to identify peptides with diGly remnants from cells stably expressing 6His-NEDD8^{R74K} under canonical or atypical NEDDylation conditions.

(B) Venn diagrams indicating the number of proteins and NEDDylation sites identified in canonical and atypical NEDDylation conditions.

(C) Table indicating examples of NEDD8 substrates identified in both modes of NEDDylation with common or distinct NEDDylation sites.

(D) Number of NEDDylation sites per protein under canonical and atypical NEDDylation conditions.

(E) NEDDylated lysines in NEDD8, ubiquitin, and SUMO-2. Common sites for canonical and atypical NEDDylation are indicated in yellow, atypical sites are indicated in red.

(F–H) Venn diagrams showing the comparison between NEDD8 sites with previously reported ubiquitin (F), SUMO sites (G), and comparison between the three modifiers (H) (Hornbeck et al., 2012).

with a differential profile of site modification (Figure 2C; Table S2). Examples for such substrates include ribosomal proteins, replication licensing factors, ubiquitin proteases, and valosin-containing protein (VCP, also known as p97 and CDC48). The vast majority of substrates have a single site of modification under both conditions of NEDDylation (Figure 2D; Table S2).

NEDDylation sites on NEDD8, ubiquitin, and SUMO were also identified in both conditions, indicating the formation of poly-NEDD8, hybrid NEDD8-ubiquitin, and NEDD8-SUMO chains (Figure 2E). This is consistent with the emerging concept of the cross-talk of ubiquitin/Ubls, especially under proteotoxic stress conditions, and with the role of poly-NEDD8 chains as regulatory molecular signal (Abidi and Xirodimas, 2015; Bailly et al., 2019; Hendriks and Vertegaal, 2016; Keuss et al., 2019; Li et al., 2015; Maghames et al., 2018).

We compared the identified NEDD8 sites with those previously reported for ubiquitin and SUMO (Hornbeck et al., 2012). A high overlap between NEDD8 and ubiquitin (60% of total NEDD8 sites) is observed (Figure 2F; Table S2). These sites were previously reported as ubiquitin sites based on the use of anti-diGly antibodies upon trypsin digestion, which, as discussed earlier, cannot discriminate between ubiquitin and NEDD8 conjugation. Thus, our data suggest that these sites rather represent NEDDylation sites or possibly that different pools of a substrate are modified either by NEDD8 or ubiquitin on the same lysine, examples of which have been reported previously (Abidi and Xirodimas, 2015). There are 485 NEDD8 sites, mainly representing NEDD8 modifications under canonical conditions, which were not identified in previous diGly studies. This is most likely due to the fact that, in our study, canonical NEDDylation was enhanced (NEDP1 knockout). Overlap between NEDDylation and SUMOylation sites was also observed (10% of total NEDD8 sites), consistent with recent studies reporting the mutually exclusive modification of substrates either with NEDD8 or SUMO (Figure 2G; Table S2) (El Motiam et al., 2019). Modification of the same lysine by all three modifiers is also observed for 115 sites, indicating the extensive cross-talk between ubiquitin and Ubls for the control of protein function (Figure 2H; Table S2).

Gene Ontology enrichment analysis revealed that the canonical pathway may be involved in the control of the spliceosome, DNA replication, mRNA surveillance pathways, and RNA transport, whereas the atypical pathway may be involved in the regulation of the ribosome, proteasome, and translation (Figure 3A; Table S3). A striking finding of the functional association analysis is that canonical and atypical NEDDylation modify distinct clusters of substrates that are functionally linked (Figures 3B and 3C; Table S3). Characteristic examples include spliceosome components (canonical), which are functionally linked to ribosome subunits (atypical) (Figure 3B). Thus, atypical and canonical NEDDylation may be functionally linked through the modification of distinct groups of substrates.

Vogl and colleagues recently reported a similar strategy for the identification of NEDD8 sites by introducing an R74K mutation on the endogenous NEDD8 gene in cells deleted of NEDP1 (canonical) (Vogl et al., 2020). Comparison of the 1,101 sites reported here with the 610 sites reported by Vogl et al. identifies 158 common sites (Figure S3; Table S4). The vast majority of these sites (141) were identified upon NEDP1 knockout (canonical), further supporting the idea for the presence of distinct proteomes for canonical and atypical NEDDylation. Gene Ontology enrichment analysis for the sites identified in both studies indicates that control of nuclear-related processes such as DNA replication and chromosome organization may be key functions of canonical NEDDylation (Figure S3; Table S4).

Formation of NEDD8-SUMO-2 Chains upon Proteotoxic Stress (Atypical NEDDylation) Mainly through K11 of SUMO-2

The proteomic data indicate the generation of NEDD8-SUMO-2 hybrid chains through NEDDylation of multiple SUMO-2 lysine residues mainly upon conditions of atypical NEDDylation (Figure 2E). To test the formation of such conjugates, we isolated, under denaturing conditions, 6His-NEDDylated proteins from cells exposed to proteotoxic stress (treatment with MG132 or heat shock). Western blot analysis using an anti-SUMO-2 antibody shows the generation of NEDD8-SUMO conjugates specifically upon proteotoxic stress (Figure 4A). Based on the identified NEDDylation sites on SUMO-2, we tested the NEDD8-SUMO-2 conjugation using several SUMO-2 lysine mutants (K11R, K21R, K33R, and K35R) upon proteotoxic stress. We expressed either wild-type or KR 6His-SUMO-2 mutants in control and stressed HCT116 cells and isolated 6His-SUMO-2 conjugates under denaturing conditions. Among the tested SUMO-2 KR mutants, the K11R showed a decrease in the formation of NEDD8-SUMO-2 conjugates under proteasome inhibition and more dramatically under heat shock (Figure 4B; Figure S4). The data validate the proteomics analysis and show that K11 on SUMO-2 is the main lysine of NEDDylation upon proteotoxic stress.

The formation of hybrid NEDD8-ubiquitin chains has been previously reported and biologically characterized as regulatory signal of the nuclear protein quality control system (Leidecker et al., 2012; Li et al., 2015; Maghames et al., 2018). Stress-induced NEDD8-ubiquitin conjugates accumulate specifically in nuclear inclusions that contain nucleolar proteins (mainly, ribosomal proteins), but intriguingly, other key nucleolar components such as fibrillarin and nucleolin are excluded. It is suggested that proteotoxic stress causes a dramatic reorganization of the nucleolar proteome, leading to the formation of the so-called nucleolus-related inclusions (Latonen, 2019; Maghames et al., 2018). Fractionation of cell extracts shows that proteotoxic stress (MG132 or heat shock) induces the accumulation of NEDD8 and SUMO-2 conjugates in the insoluble pellet fraction (Figure 4C). Immunofluorescence analysis shows that MG132 causes the colocalization of NEDD8 and SUMO-2, specifically in nuclear structures (Figure 4D). Similarly to what is reported for NEDD8-ubiquitin conjugates, the nucleolar marker fibrillarin is excluded from SUMO-2-stained inclusions, indicating that NEDD8-SUMO-2 conjugates do not localize within the nucleolus but, rather, in the previously described nucleolus-related inclusions (Maghames et al., 2018) (Figure 4D).

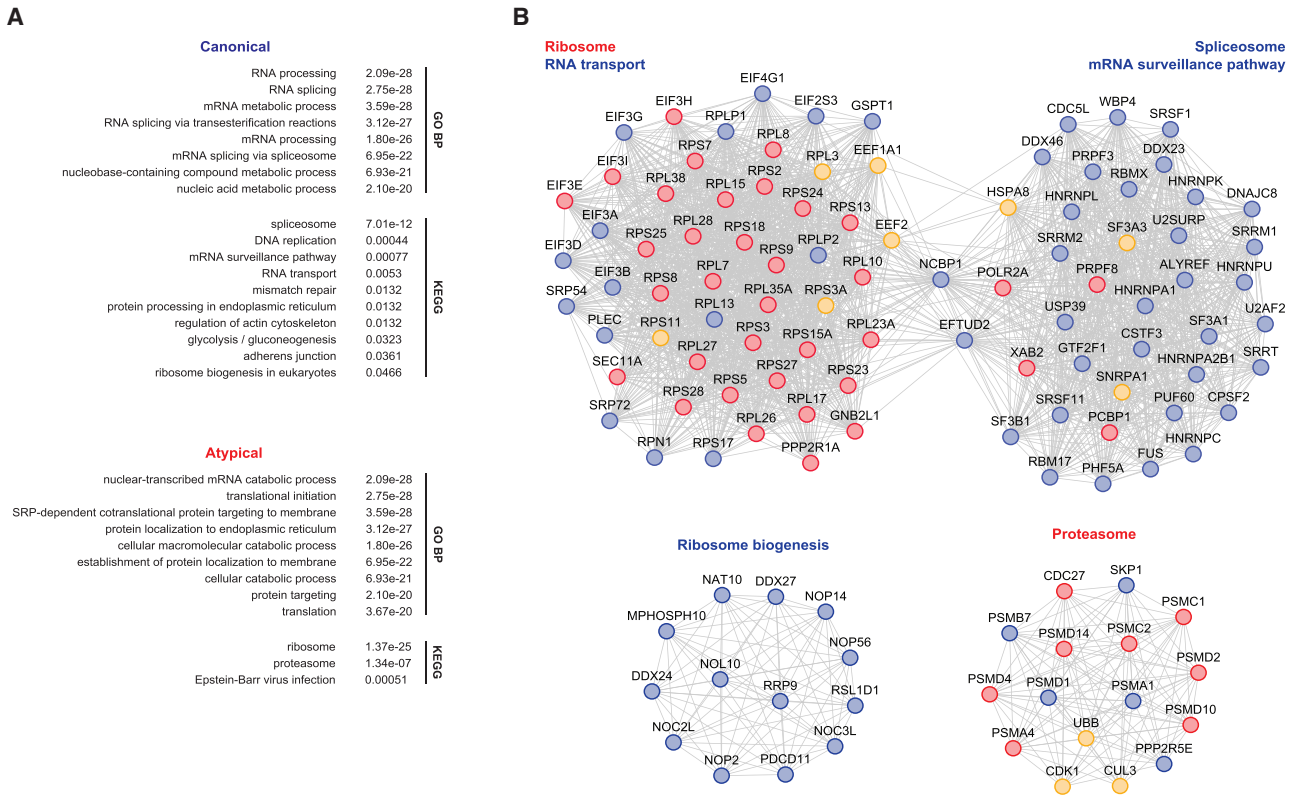

C

Category	Classification	Gene name	Function	NEDDylated sites
19S RP (PA700)	Lid	Rpn11, PSMD14	DUB	K215, K273
	Base (ATPase subunits)	Rpt1, PSMC2	ATPase	K422
		Rpt2, PSMC1	ATPase, Gate opening	K178
	Base (non-ATPase subunits)	Rpn1, PSMD2	PIPs scaffold	K397
		Rpn2, PSMD1	PIPs scaffold	K310
		Rpn10, PSMD4	Ub receptor	K135
		Rpn13, ADRM1	Ub receptor, UCHL5 recruit	K34
20S CP	α type subunits	α2, PSMA2		K165
		α3, PSMA4		K210
		α6, PSMA1		K256
PIPs		p28, PSMD10	Shuttling factor	K23
		UBQLN1	Shuttling factor	K47

Figure 3. Biological processes controlled by canonical and atypical NEDDylation

(A) Analysis of KEGG pathways and biological processes for NEDDylated proteins identified under canonical or atypical NEDDylation conditions.

(B) Functional association analysis for selected NEDD8 substrates (canonical or atypical NEDDylation).

(C) Table indicating NEDDylation sites identified under canonical (blue) or atypical (red) conditions on proteasome subunits.

DISCUSSION

Distinct proteomes for canonical and atypical NEDDylation

Identification of modification sites for ubiquitin and Ubls is an essential step toward deciphering the molecular basis of their regulatory functions. The NEDD8 pathway has an established role in the control of homeostatic and stress-response processes. A particularly intriguing aspect in protein NEDDylation is the use of distinct modes of activation and conjugation that define the canonical and atypical pathways (Abidi and Xirodimas, 2015).

Here, we report the identification of 1,101 unique NEDDylation sites on 620 proteins under canonical and atypical NEDDylation conditions. Strikingly, these two modes of NEDDylation modify distinct proteomes and, most likely, regulate different biological processes. Consistent with recent NEDD8 proteomics studies, our results indicate that major functional groups for the canonical pathway include components of the spliceosome, DNA replication, mRNA surveillance, and RNA transport (Vogl et al., 2020). For atypical NEDDylation, modified proteins are particularly enriched for processes involved in the cellular response to proteotoxic stress and regulation of proteostasis. Interestingly, NEDDylation sites on the HECT E3-ligase HUWE1, which is required for ubiquitination and atypical NEDDylation of ribosomal proteins (Maghames et al., 2018; Sung et al., 2016), were found only under atypical conditions (Table S1). This strengthens the concept that atypical NEDDylation operates mainly under proteotoxic

CellPress
OPEN ACCESS

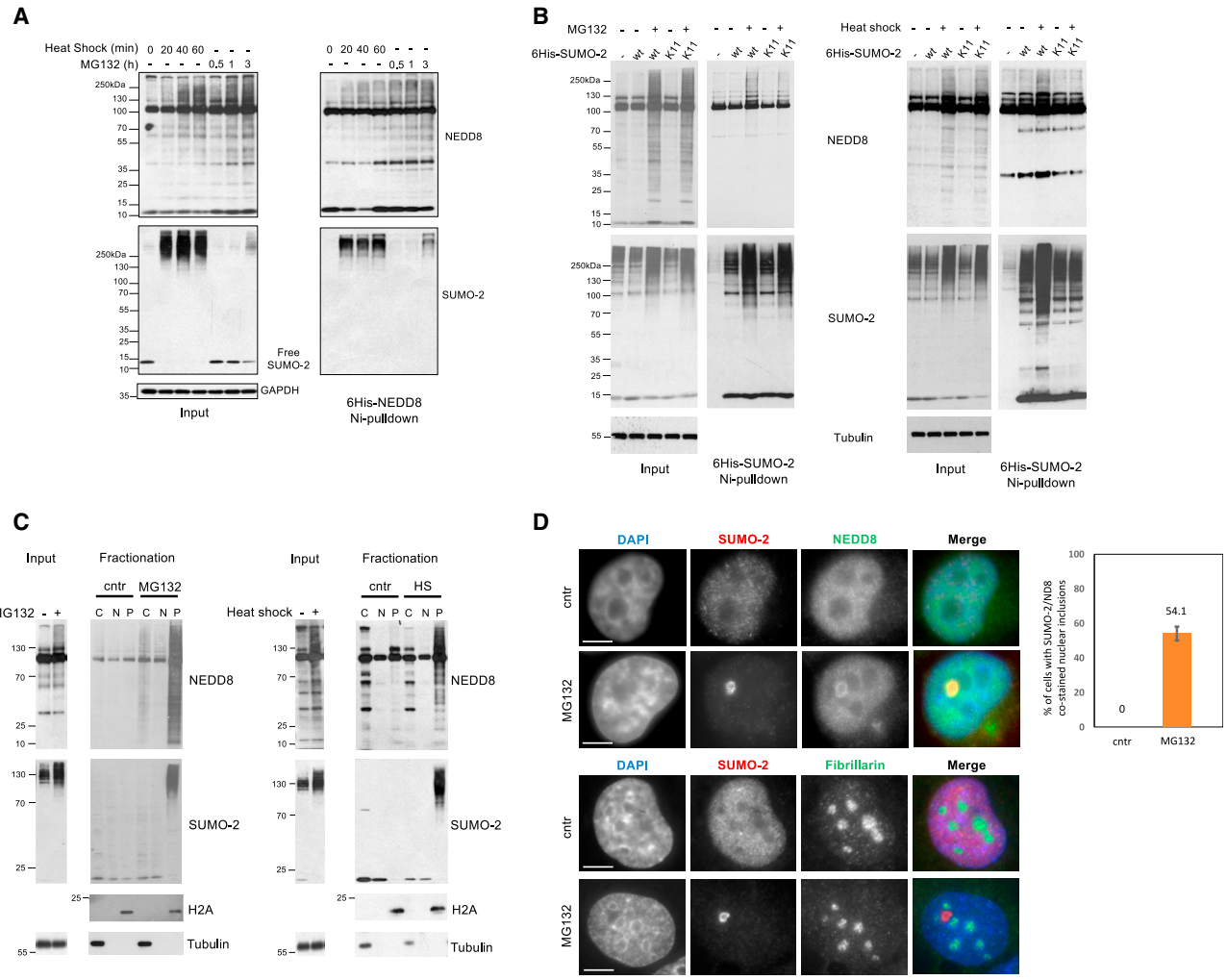

Figure 4. SUMO-2 is NEDDylated mainly on K11 upon proteotoxic stress, leading to the formation of hybrid NEDD8-SUMO-2 chains in nucleolus-related inclusions

(A) Cells stably expressing 6His-NEDD8 were exposed to proteotoxic stress (heat shock or MG132 treatment) as indicated. Isolated 6His-NEDD8 conjugates and total cell extracts (inputs) were used for western blotting.

(B) Experiment was performed as in (A), transfecting instead cells with either wild-type or K11R 6His-SUMO-2 constructs. Isolated 6His-SUMO-2 conjugates and total cell extracts were used for western blotting.

(C) Untreated or cells exposed to proteotoxic stress (MG132-30 μM, 4 h; heat shock, 43°C, 1 h) were used for subcellular fractionation and western blot analysis. C, cytoplasm; N, nucleoplasm; P, pellet. Tubulin and histone H2A were used as fractionation markers.

(D) Top: control (DMSO) or MG132-treated (5 μM, 15 h) H1299 cells (preferred system as large nuclear inclusions are formed) were used for immunofluorescence analysis for SUMO-2 (red) and NEDD8 (green). Nuclei were stained with DAPI (blue). Graph indicates the percentage of cells with nuclear inclusions co-stained with SUMO-2 and NEDD8. Data are represented as the mean of three independent experiments ± SD. Approximately 50 cells per condition were counted. Bottom: experiment performed as described above and cells stained for SUMO-2 (red) or for fibrillarin (green). Scale bars, 5 μm.

stress conditions, possibly regulating the function of E3-ligases.

For both modes of NEDDylation, multiple proteins belonging to the same functional group were identified as substrates, suggesting that, similarly to SUMO, the NEDD8 pathway may regulate processes through group modification (Psakhye and Jentsch, 2012). Examples of potential group NEDDylation include the spliceosome/ribosome biogenesis (canonical), the ribosome (atypical), and the proteasome; many ribosomal proteins and proteasome subunits were identified as targets mainly for the atypical pathway (Figures 3B and 3C). Intriguingly, recent studies revealed that proteasomes accumulate in hyperosmotic-stress-induced nuclear foci that predominantly degrade unassembled ribosomal proteins (Yasuda et al., 2020). Based on our proteomic findings and the proposed role of atypical NEDDylation in controlling, specifically, the nuclear UPS (Li et al., 2015; Maghames et al., 2018), atypical NEDDylation may be directly involved in the nuclear proteasomal degradation of unassembled ribosomal proteins (Maghames et al., 2018).

Diversity between the two modes of NEDDylation was also observed at the modification site level for common targets. In such cases, the same substrate was modified at different lysines under the two modes of NEDDylation. This indicates the distinct specificity of the enzymes involved in canonical and atypical NEDDylation for lysine preference on substrates. It remains to be revealed whether the observed diversity for lysine usage on the same target reflects distinct biological outcomes for the two modes of NEDDylation.

Diverse poly-NEDD8 and hybrid NEDD8 chains as potential molecular signals-hybrid NEDD8-SUMO chains in the proteotoxic stress response

We found that almost all lysines in NEDD8 and in ubiquitin, and many in SUMO, are NEDDylated, indicating the existence of a rather diverse range of poly-NEDD8, hybrid NEDD8-ubiquitin, or NEDD8-SUMO chains both under canonical and atypical conjugation conditions. These data support and extend previous studies that provided biological and mechanistic insights on the role of NEDD8 K11/48 chains and hybrid NEDD8-ubiquitin chains as molecular signals (Bailly et al., 2019; Li et al., 2015; Liu and Xirodimas, 2010; Maghames et al., 2018; Xirodimas et al., 2004). The present study reveals that hybrid NEDD8-SUMO-2 chains, mainly through modification of K11 in SUMO-2, participate in the response to proteotoxic stress, potentially in the formation of previously reported nucleolus-related inclusions that also contain hybrid NEDD8-ubiquitin conjugates (Maghames et al., 2018). Collectively, the data indicate the complex cross-talk of ubiquitin and Ubls in the control of the nuclear protein quality control system. The role of SUMO-2 as sensor of proteotoxic stress is well established (Castorálová et al., 2012; Tatham et al., 2011), potentially to reduce the aggregation of modified targets (Liebelt et al., 2019). In contrast, NEDD8 was proposed to promote the transient aggregation of substrates during the proteotoxic stress response (Maghames et al., 2018). It is, therefore, likely that the generation of hybrid NEDD8-SUMO-2 chains generates a new signal with altered aggregation properties for the modified targets. Based on the presented immunofluorescence analysis, NEDD8 may promote nuclear aggregation of a subset of SUMO-2-modified proteins. Defining the NEDD8-SUMO-2 sub-proteome may provide insights on the role of hybrid NEDD8-SUMO-2 chains in protein quality control.

These findings strengthen the growing concept for an extensive cross-talk between ubiquitin and Ubls to control protein function, particularly in proteotoxic stress conditions (Abidi and Xirodimas, 2015; Hendriks and Vertegaal, 2016; Tatham et al., 2011). The formation of NEDD8 polymers through distinct lysine residues may be a key aspect through which the NEDD8 pathway controls protein function and signaling. The NEDD8 pathway is regarded as a promising target for therapeutic intervention, and inhibitors of the canonical NEDD8 pathway are in clinical trials (Abidi and Xirodimas, 2015). The findings that the canonical and atypical NEDD8 pathways have distinct proteomes and the existence of an extensive cross-talk between NEDD8 and ubiquitin/SUMO pathways raise the prospect of using NAE, UAE, and/or SAE (SUMO-activating enzyme) inhibitors in combination as therapeutic approaches (Abidi and Xirodimas, 2015; He et al., 2017; Hyer et al., 2018; Kumar et al., 2016; Soucy et al., 2009).

STAR★METHODS

Detailed methods are provided in the online version of this paper and include the following:

- KEY RESOURCES TABLE
- RESOURCE AVAILABILITY
  - Lead Contact
  - Materials Availability
  - Data and Code Availability
- EXPERIMENTAL MODEL AND SUBJECT DETAILS
- METHOD DETAILS
  - Generation of NEDP1 knockout HCT116 cells by CRISPR/CAS9
  - Generation of stable cell lines by lentivirus-based approach
  - Transfections
  - Subcellular fractionation
  - Immunofluorescence microscopy
  - Isolation of 6His-NEDD8/SUMO-2 conjugates by Ni-NTA pulldowns
  - Western blot analysis
  - Sample preparation and mass spectrometry analysis
  - Bioinformatics analysis
- QUANTIFICATION AND STATISTICAL ANALYSIS

SUPPLEMENTAL INFORMATION

Supplemental information can be found online at https://doi.org/10.1016/j.celrep.2020.108635.

ACKNOWLEDGMENTS

We are grateful to Dr. Guillaume Bossis, Dr. Rivas Vazquez, and Dr. Ronald T. Hay for SUMO-2 reagents and the Montpellier Rio Imaging (MRI) facility for the microscopy. The study was supported by an ATIP/Avenir fellowship awarded to D.P.X.; the Emmy Noether Program (BE 5342/1-1) and German Research Foundation award SFB1177 to P.B.; and the Prematuration program Ubipièges funded by the Occitanie region, France, awarded to M.S.R. and D.P.X. S.L.-G. was supported by a PhD fellowship awarded by CONACYT and C.M. and L.B. were supported by Labex EpiGenMed, an "(Investissements d'avenir" program, reference ANR-10-LABEX-12-01.

AUTHOR CONTRIBUTIONS

S.L.-G. performed all the biology, cell extract preparation, and bioinformatics analyses. J.B.H. performed the sample preparation, anti-diGly immunoprecipitations, mass spectrometry, and bioinformatics analysis. C.M., L.B., and A.B. performed the experiments regarding the characterization of NEDD8-SUMO-2 hybrid chains. D.P.X., P.B., and M.S.R. supervised the work. D.P.X. wrote the manuscript, with the help of all authors.

DECLARATION OF INTERESTS

The authors declare no competing interests.

Received: January 21, 2020
Revised: November 20, 2020
Accepted: December 21, 2020
Published: January 19, 2021

REFERENCES

Abidi, N., and Xirodimas, D.P. (2015). Regulation of cancer-related pathways by protein NEDDylation and strategies for the use of NEDD8 inhibitors in the clinic. Endocr. Relat. Cancer *22*, T55–T70.

Bailly, A.P., Perrin, A., Serrano-Macia, M., Maghames, C., Leidecker, O., Trauchessec, H., Martinez-Chantar, M.L., Gartner, A., and Xirodimas, D.P. (2019). The Balance between Mono- and NEDD8-Chains Controlled by NEDP1 upon DNA Damage Is a Regulatory Module of the HSP70 ATPase Activity. Cell Rep. *29*, 212–224.e8.

Brockmann, M.M., Döngi, M., Einsfelder, U., Körber, N., Refojo, D., and Stein, V. (2019). Neddylation regulates excitatory synaptic transmission and plasticity. Sci. Rep. *9*, 17935.

Castorálová, M., Březinová, D., Svéda, M., Lipov, J., Ruml, T., and Knejzlík, Z. (2012). SUMO-2/3 conjugates accumulating under heat shock or MG132 treatment result largely from new protein synthesis. Biochim. Biophys. Acta *1823*, 911–919.

Chen, C., Li, Z., Huang, H., Suzek, B.E., and Wu, C.H.; UniProt Consortium (2013). A fast Peptide Match service for UniProt Knowledgebase. Bioinformatics *29*, 2808–2809.

Cox, J., and Mann, M. (2008). MaxQuant enables high peptide identification rates, individualized p.p.b.-range mass accuracies and proteome-wide protein quantification. Nat. Biotechnol. *26*, 1367–1372.

El Motiam, A., Vidal, S., de la Cruz-Herrera, C.F., Da Silva-Álvarez, S., Baz-Martínez, M., Seoane, R., Vidal, A., Rodríguez, M.S., Xirodimas, D.P., Carvalho, A.S., et al. (2019). Interplay between SUMOylation and NEDDylation regulates RPL11 localization and function. FASEB J. *33*, 643–651.

Enchev, R.I., Schulman, B.A., and Peter, M. (2015). Protein neddylation: beyond cullin-RING ligases. Nat. Rev. Mol. Cell Biol. *16*, 30–44.

He, X., Riceberg, J., Soucy, T., Koenig, E., Minissale, J., Gallery, M., Bernard, H., Yang, X., Liao, H., Rabino, C., et al. (2017). Probing the roles of SUMOylation in cancer cell biology by using a selective SAE inhibitor. Nat. Chem. Biol. *13*, 1164–1171.

Hendriks, I.A., and Vertegaal, A.C.O. (2016). A comprehensive compilation of SUMO proteomics. Nat. Rev. Mol. Cell Biol. *17*, 581–595.

Hjerpe, R., Thomas, Y., Chen, J., Zemla, A., Curran, S., Shpiro, N., Dick, L.R., and Kurz, T. (2012). Changes in the ratio of free NEDD8 to ubiquitin triggers NEDDylation by ubiquitin enzymes. Biochem. J. *441*, 927–936.

Hornbeck, P.V., Kornhauser, J.M., Tkachev, S., Zhang, B., Skrzypek, E., Murray, B., Latham, V., and Sullivan, M. (2012). PhosphoSitePlus: a comprehensive resource for investigating the structure and function of experimentally determined post-translational modifications in man and mouse. Nucleic Acids Res. *40*, D261–D270.

Hyer, M.L., Milhollen, M.A., Ciavarri, J., Fleming, P., Traore, T., Sappal, D., Huck, J., Shi, J., Gavin, J., Brownell, J., et al. (2018). A small-molecule inhibitor of the ubiquitin activating enzyme for cancer treatment. Nat. Med. *24*, 186–193.

Keuss, M.J., Hjerpe, R., Hsia, O., Gourlay, R., Burchmore, R., Trost, M., and Kurz, T. (2019). Unanchored tri-NEDD8 inhibits PARP-1 to protect from oxidative stress-induced cell death. EMBO J. *38*, e100024.

Kim, W., Bennett, E.J., Huttlin, E.L., Guo, A., Li, J., Possemato, A., Sowa, M.E., Rad, R., Rush, J., Comb, M.J., et al. (2011). Systematic and quantitative assessment of the ubiquitin-modified proteome. Mol. Cell *44*, 325–340.

Kumar, A., Ito, A., Hirohama, M., Yoshida, M., and Zhang, K.Y.J. (2016). Identification of new SUMO activating enzyme 1 inhibitors using virtual screening and scaffold hopping. Bioorg. Med. Chem. Lett. *26*, 1218–1223.

Latonen, L. (2019). Phase-to-Phase With Nucleoli - Stress Responses, Protein Aggregation and Novel Roles of RNA. Front. Cell. Neurosci. *13*, 151.

Leidecker, O., Matic, I., Mahata, B., Pion, E., and Xirodimas, D.P. (2012). The ubiquitin E1 enzyme Ube1 mediates NEDD8 activation under diverse stress conditions. Cell Cycle *11*, 1142–1150.

Li, T., Guan, J., Huang, Z., Hu, X., and Zheng, X. (2014). RNF168-mediated H2A neddylation antagonizes ubiquitylation of H2A and regulates DNA damage repair. J. Cell Sci. *127*, 2238–2248.

Li, J., Ma, W., Li, H., Hou, N., Wang, X., Kim, I.M., Li, F., and Su, H. (2015). NEDD8 Ultimate Buster 1 Long (NUB1L) Protein Suppresses Atypical Neddylation and Promotes the Proteasomal Degradation of Misfolded Proteins. J. Biol. Chem. *290*, 23850–23862.

Liebelt, F., Sebastian, R.M., Moore, C.L., Mulder, M.P.C., Ovaa, H., Shoulders, M.D., and Vertegaal, A.C.O. (2019). SUMOylation and the HSF1-Regulated Chaperone Network Converge to Promote Proteostasis in Response to Heat Shock. Cell Rep. *26*, 236–249.e4.

Liu, G., and Xirodimas, D.P. (2010). NUB1 promotes cytoplasmic localization of p53 through cooperation of the NEDD8 and ubiquitin pathways. Oncogene *29*, 2252–2261.

Ma, T., Chen, Y., Zhang, F., Yang, C.-Y., Wang, S., and Yu, X. (2013). RNF111-dependent neddylation activates DNA damage-induced ubiquitination. Mol. Cell *49*, 897–907.

Maghames, C.M., Lobato-Gil, S., Perrin, A., Trauchessec, H., Rodriguez, M.S., Urbach, S., Marin, P., and Xirodimas, D.P. (2018). NEDDylation promotes nuclear protein aggregation and protects the Ubiquitin Proteasome System upon proteotoxic stress. Nat. Commun. *9*, 4376.

Mergner, J., Heinzlmeir, S., Kuster, B., and Schwechheimer, C. (2015). DENEDDYLASE1 deconjugates NEDD8 from non-cullin protein substrates in *Arabidopsis thaliana*. Plant Cell *27*, 741–753.

Ordureau, A., Münch, C., and Harper, J.W. (2015). Quantifying ubiquitin signaling. Mol. Cell *58*, 660–676.

Psakhye, I., and Jentsch, S. (2012). Protein group modification and synergy in the SUMO pathway as exemplified in DNA repair. Cell *151*, 807–820.

Rappsilber, J., Mann, M., and Ishihama, Y. (2007). Protocol for micro-purification, enrichment, pre-fractionation and storage of peptides for proteomics using StageTips. Nat. Protoc. *2*, 1896–1906.

Schneider, C.A., Rasband, W.S., and Eliceiri, K.W. (2012). NIH Image to ImageJ: 25 years of image analysis. Nat. Methods *9*, 671–675.

Shannon, P., Markiel, A., Ozier, O., Baliga, N.S., Wang, J.T., Ramage, D., Amin, N., Schwikowski, B., and Ideker, T. (2003). Cytoscape: a software environment for integrated models of biomolecular interaction networks. Genome Res. *13*, 2498–2504.

Soucy, T.A., Smith, P.G., Milhollen, M.A., Berger, A.J., Gavin, J.M., Adhikari, S., Brownell, J.E., Burke, K.E., Cardin, D.P., Critchley, S., et al. (2009). An inhibitor of NEDD8-activating enzyme as a new approach to treat cancer. Nature *458*, 732–736.

Sung, M.-K., Porras-Yakushi, T.R., Reitsma, J.M., Huber, F.M., Sweredoski, M.J., Hoelz, A., Hess, S., and Deshaies, R.J. (2016). A conserved quality-control pathway that mediates degradation of unassembled ribosomal proteins. eLife *5*, e19105.

Szklarczyk, D., Franceschini, A., Wyder, S., Forslund, K., Heller, D., Huerta-Cepas, J., Simonovic, M., Roth, A., Santos, A., Tsafou, K.P., et al. (2015). STRING v10: protein-protein interaction networks, integrated over the tree of life. Nucleic Acids Res. *43*, D447–D452.

Tammsalu, T., Matic, I., Jaffray, E.G., Ibrahim, A.F.M., Tatham, M.H., and Hay, R.T. (2014). Proteome-wide identification of SUMO2 modification sites. Sci. Signal. *7*, rs2.

Tatham, M.H., Rodriguez, M.S., Xirodimas, D.P., and Hay, R.T. (2009). Detection of protein SUMOylation in vivo. Nat. Protoc. *4*, 1363–1371.

Tatham, M.H., Matic, I., Mann, M., and Hay, R.T. (2011). Comparative proteomic analysis identifies a role for SUMO in protein quality control. Sci. Signal. *4*, rs4.

Vogl, A.M., Brockmann, M.M., Giusti, S.A., Maccarrone, G., Vercelli, C.A., Bauder, C.A., Richter, J.S., Roselli, F., Hafner, A.-S., Dedic, N., et al. (2015). Neddylation inhibition impairs spine development, destabilizes synapses and deteriorates cognition. Nat. Neurosci. *18*, 239–251.

Vogl, A.M., Phu, L., Becerra, R., Giusti, S.A., Verschueren, E., Hinkle, T.B., Bordenave, M.D., Adrian, M., Heidersbach, A., Yankilevich, P., et al. (2020). Global site-specific neddylation profiling reveals that NEDDylated cofilin regulates actin dynamics. Nat. Struct. Mol. Biol. *27*, 210–220.

Wagner, S.A., Beli, P., Weinert, B.T., Nielsen, M.L., Cox, J., Mann, M., and Choudhary, C. (2011). A Proteome-wide, Quantitative Survey of In Vivo

Ubiquitylation Sites Reveals Widespread Regulatory Roles. Mol. Cell. Proteomics *10*, M111.013284.

Xirodimas, D., Saville, M.K., Edling, C., Lane, D.P., and Laín, S. (2001). Different effects of p14ARF on the levels of ubiquitinated p53 and Mdm2 in vivo. Oncogene *20*, 4972–4983.

Xirodimas, D.P., Saville, M.K., Bourdon, J.-C., Hay, R.T., and Lane, D.P. (2004). Mdm2-mediated NEDD8 conjugation of p53 inhibits its transcriptional activity. Cell *118*, 83–97.

Xirodimas, D.P., Sundqvist, A., Nakamura, A., Shen, L., Botting, C., and Hay, R.T. (2008). Ribosomal proteins are targets for the NEDD8 pathway. EMBO Rep. *9*, 280–286.

Xu, G., Paige, J.S., and Jaffrey, S.R. (2010). Global analysis of lysine ubiquitination by ubiquitin remnant immunoaffinity profiling. Nat. Biotechnol. *28*, 868–873.

Yasuda, S., Tsuchiya, H., Kaiho, A., Guo, Q., Ikeuchi, K., Endo, A., Arai, N., Ohtake, F., Murata, S., Inada, T., et al. (2020). Stress- and ubiquitylation-dependent phase separation of the proteasome. Nature *578*, 296–300.

STAR★METHODS

KEY RESOURCES TABLE

REAGENT or RESOURCE	SOURCE	IDENTIFIER
Antibodies		
Rabbit monoclonal anti-NEDD8, Y297	GeneTex	Cat#GTX61205; RRID:AB_10619223
Rabbit anti-ubiquitin, western blotting	DAKO	Cat#z0458; RRID:AB_2315524
Mouse anti-GAPDH (C65)	Abcam	Cat#ab8245; RRID:AB_2107448
Rabbit anti-UBA3	Abcam	Cat#ab124728; RRID:AB_10974248
Rabbit anti-UBA1	Abcam	Cat#ab34711; RRID:AB_742233
Rabbit anti-Histone H2A	Abcam	Cat#ab13923; RRID:AB_300750
Rabbit anti-Fibrillarin	Abcam	Cat#ab5821; RRID:AB_2105785
Rabbit anti-Histone H2B	Millipore	Cat#Ab1623; RRID:AB_2118289
Ubiquitin Branch Motif Antibody (K-ε-GG)	Cell Signaling	Cat#5562
Mouse anti-Tubulin	Cell Signaling	Cat#86298; RRID:AB_2715541
Mouse anti-APPBP1	Abnova	Cat#H00008883-M01; RRID:AB_536865
Mouse anti-SUMO-2 antibody	DSHB	Cat#8A2; RRIR:AB_2198421
Alexa goat anti-mouse 488	Jackson ImmunoResearch	Cat#115-545-003; RRID:AB_2338840
Alexa goat anti-rabbit 594	Jackson ImmunoResearch	Cat#111-585-144; RRID:AB_2307325
Chemicals, Peptides, and Recombinant Proteins		
MLN4924	Active Biochem	A-1139
MLN7243	Chemietek	AOB 87172
Endopeptidase LysC	FUJIFILM Wako Pure Chemical Corporation	125-05061
4-12% Bis-Tris gels	Invitrogen	NP0322
Compounds	Sigma Aldrich	N/A
Fugene6 HD	Roche	11814443001
Protease Inhibitor Cocktail Tablets EDTA-free	Roche	11873580001
Ni-NTA Agarose	QIAGEN	30210
PVDF membrane	Millipore	IPVH00010
ECL Western Blotting Detection Reagents	Amersham	RPN2106
Protein G Sepharose beads	Amersham	17061801
Medical X-ray films	Konica	A9KN
Deposited Data		
Deposition of mass spectrometry proteomics data	PRIDE ProteomeXchange Consortium	PXD022812
Experimental Models: Cell Lines		
Human: HCT116	ATCC	CCL-247
Human: H1299	ATCC	CRL-5803
Oligonucleotides		
ON-TARGETplus Human UBA1 siRNA	Dharmacon	L-004509-00-0005
ON-TARGETplus Human APPBP1 siRNA	Dharmacon	L-006401-00-0005
ON-TARGETplus Human UBA3 siRNA	Dharmacon	L-005249-00-0005
Recombinant DNA		
His_6-NEDD8 wt	Xirodimas et al., 2001	N/A
His_6-NEDD8 R74K	This paper	N/A
His_6-SUMO-2 wt	Dr Rivas Vazquez, CIMUS, Spain	N/A
His_6-SUMO-2 K11R	Dr Rivas Vazquez, CIMUS, Spain	N/A
His_6-SUMO-2 K21R, K33R, K35R	This study	N/A

(*Continued on next page*)

Continued

REAGENT or RESOURCE	SOURCE	IDENTIFIER
Software and Algorithms		
MaxQuant 1.5.2.8	Cox and Mann, 2008	https://www.maxquant.org
UniProtKB	Chen et al., 2013	https://www.uniprot.org/help/uniprotkb
STRING database	Szklarczyk et al., 2015	N/A
Cytoscape 3.4.0	Shannon et al., 2003	N/A
PhosphoSitePlus	Hornbeck et al., 2012	N/A
ImageJ	Schneider et al., 2012	N/A

RESOURCE AVAILABILITY

Lead Contact

Further information and requests for resources and reagents should be directed to and will be fulfilled by the Lead Contact, Dimitris P. Xirodimas (dimitris.xirodimas@crbm.cnrs.fr) and co-corresponding author Petra Beli (p.beli@imb-mainz.de).

Materials Availability

Plasmids and cell lines newly generated in this study will be made readily available to the scientific community. We will honor requests in a timely fashion.

Data and Code Availability

The accession number for the mass spectrometry proteomics data reported in this paper is: ProteomeXchange Consortium via the PRIDE partner with the dataset identifier PXD022812.

EXPERIMENTAL MODEL AND SUBJECT DETAILS

HCT116 cells (Male) and H1299 lung carcinoma cells (Male) were cultured in Dulbecco's modified Eagle's (DMEM) and RPMI medium respectively supplemented with 10% fetal bovine serum (FBS) and standard antibiotics (Penicillin, 50 U/ml and Streptomycin 50μg/ml) in 5% CO2 at 37°C in a humidified incubator. HCT116 cells stably expressing 6His-NEDD8^{WT} or 6His-NEDD8^{R74K} were cultured in the presence of 2.5 μM puromycin for selection. The cell lines have not been authenticated but routinely checked for mycoplasma contamination.

METHOD DETAILS

Generation of NEDP1 knockout HCT116 cells by CRISPR/CAS9

HCT116 cells seeded in 10cm Petri dishes were transfected with 6 μg of gRNA-NEDP1-Cas9-GFP vector (Sigma-Aldrich) with Fugene 6 HD (Roche) (Bailly et al., 2019). 24hrs post transfection cells were subjected to fluorescence-activated cell sorting (FACS) to isolate GFP positive cells. Cell clones were tested for NEDP1 depletion and high levels of NEDD8 protein levels by western blot analysis and selected for further experiments.

Generation of stable cell lines by lentivirus-based approach

6His-NEDD8^{WT} and 6His-NEDD8^{R74K} mutant were cloned into lentivirus vector (sequences confirmed) and virus was produced as described in Liu and Xirodimas, 2010. Parental and NEDP1 knockout (C8) HCT116 cells were seeded in 6-well plates and 200 μL of the lentiviral supernatant was added to the cells in the presence of 10 μg/ml polybrene. Medium was replaced with DMEM with 10% FBS the next day. 3 days post-infection, puromycin was added to the medium at 5 μg/ml. Stable cell lines were maintained in the medium with 2.5 μg/ml of puromycin and the expression of 6His-NEDD8 was regularly tested. Cells were kept in tissue culture for a maximum of 20 passages.

Transfections

Cells seeded in 10cm dishes were transfected with 5nM of siRNA (Dharmacon On-TARGETplus SMARTpools) using Lipofectamine RNAiMAX according to manufacturer's instructions. Non-target siRNA was used in control transfections. For NAE knockdown, siRNAs against both the catalytic (UBA3) and regulatory (APPBP1) subunits were used. Fugene6 HD Transfection Reagent was used for 6His-SUMO-2 plasmid transfections (3:1 Fugene:DNA (μg) ratio). Cells were harvested 48hrs post-transfection.

Subcellular fractionation

Experiment performed as described in Maghames et al., 2018. Briefly, cells harvested from a 10cm dish were resuspended in buffer A (10mM HEPES-KOH pH 8.0, 10mM KCl, 1.5mM $MgCl_2$, protease inhibitors, 10mM iodoacetamide). The cytoplasmic fraction was obtained by lysing cells with the addition of Triton X-100 at 0.1% for 1min at 4°C, then centrifuged for 5min at 1300 g, 4°C. After washing 3x with buffer A, the remaining pellet (nucleus) was resuspended in buffer B (20mM HEPES-KOH pH 8.0, 300mM NaCl, 2mM EDTA and 1%NP40) and incubated 30min on ice before sonication 8x30s with 30% amplitude (Branson Digital Sonifier) and centrifugation at 16200 g, 4°C, 15min. The supernatant (nucleoplasmic fraction) and the pellet (washed 3x, buffer B) were resuspended in 2xSDS.

Immunofluorescence microscopy

Cells were seeded on round coverslips 24hrs before treatment. After treatment, cells were washed 2x with warm PBS and fixed with 4% formaldehyde (5min). After washing 3x10min with warm PBS, cells were permeabilized with 1% Triton X-100 in PBS for 10min. Cells were washed 3 × 10min with PBS before blocking with 0.05% Tween-20 + 1% Goat serum in PBS for 1hr. Samples were incubated with primary antibodies diluted in 0.05% tween-20 + 1% Goat serum in PBS overnight at 4°C. After 3 × 10min washes with 0.05% Tween-20 in PBS, corresponding secondary antibodies diluted in 0.05% Tween-20 + 1% Goat serum in PBS were added for 1hr at room temperature in the dark. Samples were washed 3 × 10min with 0.05% tween-20 in PBS, and DAPI stained (1/20000) for 20 s at room temperature in the dark. Slides were washed 3x with PBS, mounted with Vectashield Mounting Medium (H-1000, Vector), sealed, and viewed under the microscope Leica DM6000 or Leica SP5-SMD using metamorph software. The images were analyzed by ImageJ64 software. SUMO-2 mouse monoclonal antibody was used at 1:250 dilution whereas NEDD8 rabbit monoclonal at 1:150. The secondary antibodies Alexa goat anti-mouse 488 and goat anti-rabbit 594 were diluted at 1:500.

Isolation of 6His-NEDD8/SUMO-2 conjugates by Ni-NTA pulldowns

After the indicated treatments/transfections, cells were washed twice with ice cold PBS and harvested in 1ml PBS by scraping. 200 μL of cells were used for direct lysis in 2xSDS laemmli whereas the remaining 800 μL were lysed in 6M GmCl, pH 8, 10mM β-mercaptoethanol, 0.1% Triton X-100, 5mM imidazole lysis buffer. Samples were sonicated 10x30s at 40% amplitude (Branson Digital Sonifier). Insoluble particles were removed by centrifugation at 13000rpm for 15min at 4°C. Protein extract was filtered with 0.2 μm sterile filters and protein concentration was determined by BCA assay. Purification of 6His-NEDD8/SUMO-2 conjugates was performed as previously described (Tatham et al., 2009; Xirodimas et al., 2001). Briefly, after overnight incubation at 4°C with 50 μL of Nickel-agarose beads, washes were performed with 500 μL of each of the following buffers: 6M GmCl, pH 8, 10mM β-mercaptoethanol, 0.1% Triton X-100 (1x), 8M Urea, pH 8, 10mM β-mercaptoethanol, 0.1% Triton X-100 (1x), 8M Urea, pH 6.3, 10mM β-mercaptoethanol, 0.1% Triton X-100 (3x). Elution was performed at room temperature, rotating 20min in 100 μL of 2xSDS Laemmli's buffer containing 250mM imidazole.

Western blot analysis

Proteins were resolved in sodium dodecyl sulfate (SDS) polyacrylamide electrophoresis (SDS-PAGE) gels and transferred onto PVDF membrane using the Bio-Rad Mini Trans-Blot apparatus. Membranes were blocked in 5% milk solution (PBS with 0.1% Tween-20 and 5% skimmed milk) for 1hr at room temperature with gentle agitation. Membranes were incubated with the primary antibodies overnight at 4°C. Primary antibodies were diluted in PBS 0.1% Tween-20 with 3% BSA and 0.1% NaN_3. Membranes were washed 3x10min with PBS 0.1% Tween-20 and then incubated with the appropriate secondary antibody (Sigma Aldrich) for 1hr at room temperature (5% milk). After incubation, membranes were washed 2x15min with PBS 0.1% Tween-20 followed by 2x5min with PBS. Detection was performed with ECL Western Blotting Detection Reagents and membranes were exposed to X-ray Medical Film before being developed.

Sample preparation and mass spectrometry analysis

Parental and NEDP1 knockout HCT116 cells stably expressing 6His-$NEDD8^{R74K}$ were washed with PBS and lysed in modified RIPA buffer (50mM Tris-HCl pH 7.5, 150mM NaCl, 1mM EDTA, 1% NP-40, 0.1% Na-deoxycholate, protease inhibitors) then incubated for 15min on ice. Lysate was sonicated for 3x30s at 30% amplitude (Branson Digital Sonifier) and cleared by centrifugation at 13000rpm for 15min. Supernatants were collected and protein concentration was measured using BCA assay. Around 200mg of proteins were precipitated overnight in 4xVol cold acetone at −20°C. Precipitated proteins were re-dissolved in denaturing buffer (6M Urea and 2M thiourea in 10mM HEPES at pH 8). Cysteines were reduced with 1mM dithiothreitol for 45min and alkylated with 5.5mM chloroacetamide for 30min in the dark. Proteins were subsequently proteolysed in 1:100 and 1:500 with endoproteinase Lys-C (Wako Chemicals) overnight. Peptides were purified using reversed-phase Sep-Pak C18 cartridges (Waters), and dissolved in immunoprecipitation buffer (10mM sodium phosphate and 50mM sodium chloride in 50mM MOPS at pH 7.2). Di-glycine-modified peptides were immuno-enriched using PTMScan® Ubiquitin Branch Motif (K-ε-GG) beads (Cell Signaling Technology). Peptides were incubated for 4hrs at 4°C on a rotation wheel. The beads were washed three times in ice-cold immunoprecipitation buffer followed by three washes in water. Immunoenriched peptides were eluted with 0.15% trifluoroacetic acid in H_2O, fractionated in six fractions using micro- column-based strong-cation exchange chromatography (SCX) and desalted on reversed phase C18 StageTips as previously described (Rappsilber et al., 2007).

Peptide fractions were analyzed on a quadrupole Orbitrap mass spectrometer (Q Exactive Plus, Thermo Scientific) equipped with a UHPLC system (EASY-nLC 1000, Thermo Scientific). Peptide samples were loaded onto C18 reversed phase columns (15cm length, 75μm inner diameter, 1.9μm bead size) and eluted with a linear gradient from 8 to 40% acetonitrile containing 0.1% formic acid in 2hrs. The mass spectrometer was operated in data dependent mode, automatically switching between MS and MS2 acquisition. Survey full scan MS spectra (m/z 300 – 1700) were acquired in the Orbitrap. The 10 most intense ions were sequentially isolated and fragmented by higher-energy C-trap dissociation (HCD). An ion selection threshold of 5,000 was used. Peptides with unassigned charge states, as well as with charge states less than +2 were excluded from fragmentation. Fragment spectra were acquired in the Orbitrap mass analyzer.

Raw data files were analyzed using MaxQuant (development version 1.5.2.8). Parent ion and MS2 spectra were searched against a database containing 88473 human protein sequences human protein sequences obtained from the UniProtKB released in December 2013 using Andromeda search engine. Spectra were searched with a mass tolerance of 6ppm in MS mode, 20ppm in HCD MS2 mode, strict Lys-C specificity and allowing up to 3 miscleavages. Cysteine carbamidomethylation was searched as a fixed modification, whereas protein N-terminal acetylation, methionine oxidation modification of cysteines (mass difference to cysteine carbamidomethylation) and di-glycine-lysine were searched as variable modifications. Site localization probabilities were determined by MaxQuant using the PTM scoring algorithm. Peptides with site localization probability above 0.75 were selected. Approximately 100 sites had a localization probability below 0.9. For all functional association analysis sites with localization probability $\geq$ 0.9 were used. The dataset was filtered based on posterior error probability (PEP) to arrive at a false discovery rate of below 1% estimated using a target-decoy approach. Di-glycine lysine modified peptides with a minimum score of 40 and delta score of 6 are reported and used for the analyses.

Bioinformatics analysis

STRING network analysis was performed using the online STRING database (Szklarczyk et al., 2015) using NEDDylated proteins as input. Protein interaction enrichment was performed based on the amount of interactions in the networks, as compared with the randomly expected amount of interactions, with both variables directly derived from the STRING database output. Visualization of the interaction network was performed using Cytoscape version 3.4.0 (Shannon et al., 2003).

For NEDDylation, SUMOylation and Ubiquitination site comparative overlap analysis, all NEDDylation sites were analyzed. All MS/MS-identified Ubiquitination sites and SUMOylation sites were extracted from PhosphoSitePlus (https://www.phosphosite.org) (Hornbeck et al., 2012). For each dataset, sites from mouse proteins were removed. Perseus software was used to generate a matrix where all proteins from all PTMs were cross-referenced to each other.

QUANTIFICATION AND STATISTICAL ANALYSIS

ImageJ, STRING network analysis, Cytoscape 3.4.0, PhosphoSitePlus, MaxQuant 1.5.2.8, UniProtKB were used. Details for the statistical tests used can be found in figure legends. Values represent the average ± SD and n values represent the number of independent experiments as indicated in figure legends. No methods were used to determine whether the data met assumptions of the statistical approach.